Supplementary information

Laser-induced immobilization of amorphous iron-phosphate/Fe_3O_4 composite on nickel foam for efficient water oxidation

Yan Zou,[a] Man Jin,[a] Dongdong Zhu,[a] and Yu-Jia Tang*[a]

[a] School of Chemistry and Materials Science, Institute of Advanced Materials and Flexible Electronics (IAMFE), Nanjing University of Information Science and Technology, 219 Ningliu Road, Nanjing, 210044, China

Email: tangyujia@nuist.edu.cn

Experimental section

S1. Chemicals and materials

Iron (III) nitrate nonahydrate ($Fe(NO_3)_3 \cdot 9H_2O$, ≥98%), cobalt nitrate hexahydrate ($Co(NO_3)_2 \cdot 6H_2O$), ammonium dihydrogen phosphate ($NH_4H_2PO_4$), and ethanol (EtOH) were purchased from Sinopharm Chemical Reagent Co. Ltd. Nickel nitrate hexahydrate ($Ni(NO_3)_2 \cdot 6H_2O$) was purchased from Aladdin. Nickel foam was purchased from Kunshan Jiayisheng Electronics Co., Ltd.

S2. Physical characterizations

Surface morphology was observed using a Gemini SEM 300 field emission scanning electron microscope (FESEM) at an accelerating voltage of 5 kV. Transmission electron microscopy (TEM) and high-resolution TEM (HRTEM) images were obtained by an FEI Tecnai G2 F30 S-Twin type electron microscope operating at 300 kV. Elemental analyses and energy dispersive X-ray (EDX) analyses were performed using an X-max Oxford detector at an accelerating voltage of 15 kV. X-ray photoelectron spectroscopy (XPS) was performed with Al Kα radiation on a scanning X-ray microprobe (Thermo Fisher Scientific Escalab Xi+). Powder X-ray diffractometer (XRD) data were collected with a Smart Lab/3kW using Cu Kα radiation.

S3. Synthesis of L-FePO on NF

30 mg of $Fe(NO_3)_3 \cdot 9H_2O$, 40 mg of $NH_4H_2PO_4$, 0.5 mL of EtOH, and 0.5 mL of DI water were mixed and ultrasonicated for 1 h to prepare the FeHP precursor. 0.2 mL of the above suspension was coated on both sides of a NF substrate with a size of 1 × 2 cm^2. The coating area was 1 × 1 cm^2. After drying at 60 °C for 20 min, the FeHP precursor on NF was laser-irradiated using a laser machine (JL-K6040, Liaocheng Julong Laser Equipment Co., Ltd.) equipped with a focused 10.6 μm CO_2 laser. The laser speed and power were set to 10 mm s^{-1} and 8 W, respectively. After the laser-induced irradiation treatment, the L-FePO composite immobilized on NF was successfully obtained. For comparison, the control samples of L-CoPO and L-NiPO on NF were prepared by laser-irradiating $Co(NO_3)_2 \cdot 6H_2O/NH_4H_2PO_4$ and

$Ni(NO_3)_2 \cdot 6H_2O/NH_4H_2PO_4$ mixture precursors, respectively.

S4. Electrochemical measurements

Electrochemical measurements were performed at room temperature using a three-electrode system on an electrochemical workstation (CHI Instruments 660E, China). The L-FePO composite on NF was directly used as a working electrode with a size of 1 × 2 cm^2 and a measurement area of 1 × 1 cm^2. A Hg/HgO electrode and a graphite rod were used as reference and counter electrodes, respectively. A 1.0 M KOH solution was used as an electrolyte. The OER performance was evaluated by linear scanning voltammetry (LSV) curves at a scan rate of 5 mV s^{-1}. Tafel plots were calculated from the corresponding LSV curves. Tafel slope was calculated as follows: $\eta = a + b \log j$, where η, a, b, and j refer to overpotential, Tafel constant, Tafel slope, and current density, respectively. Chronopotentiometric (CP) curve was recorded for 100 h at a constant current density of 100 mA cm^{-2}. All the LSV and CP curves were used after 90% iR compensation. Cyclic voltammetry (CV) curves were acquired in a potential range of 0-1 V vs. Hg/HgO at different scan rates (10, 20, 40, 60, 80, and 100 mV s^{-1}) to evaluate the double layer capacitance (C_{dl}) values. Electrochemical impedance spectroscopy (EIS) was measured at an overpotential of 300 mV from 100000 to 0.01 Hz with an amplitude of 10 mV.

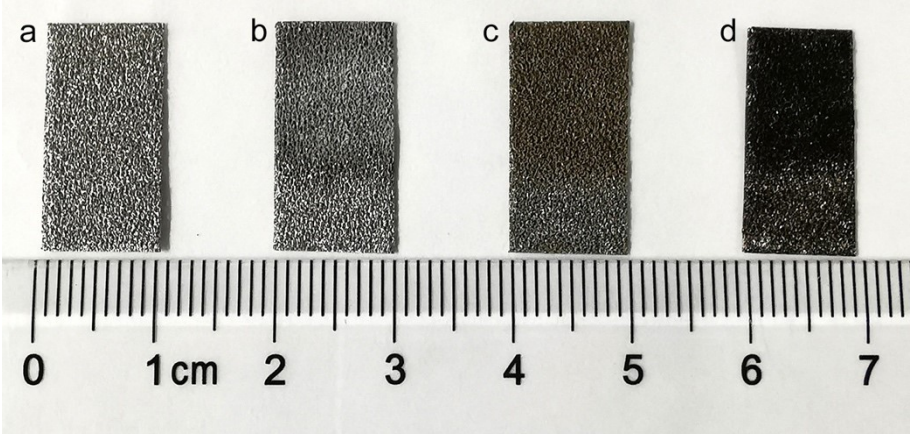

Figure S1. Photos of (a) NF, (b) FeHP precursor on NF, (c) L-FePO on NF, and (d) L-FePO on NF after the stability test for OER.

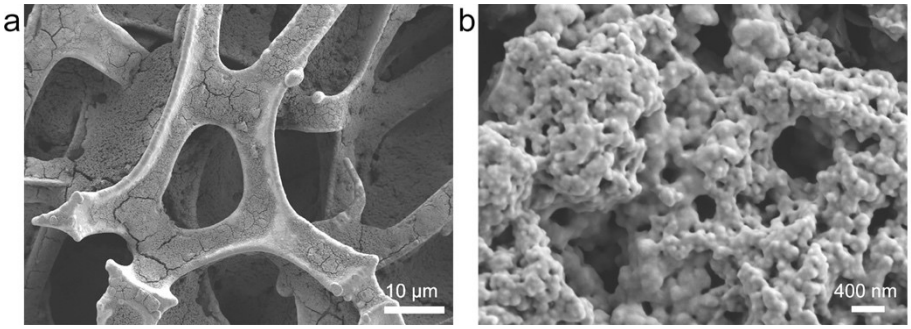

Figure S2. SEM images of the FeHP precursor loaded on NF prepared by the mixture of $Fe(NO_3)_3 \cdot 9H_2O$ and $NH_4H_2PO_4$.

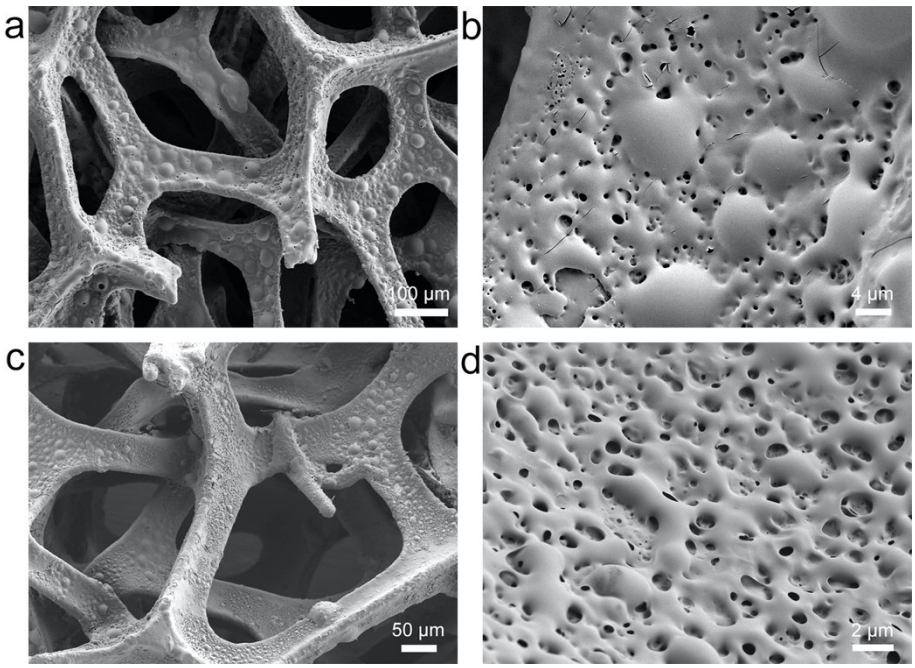

Figure S3. Low and high-magnification SEM images of L-MPO on NF: (a, b) L-CoPO, and (c, d) L-NiPO.

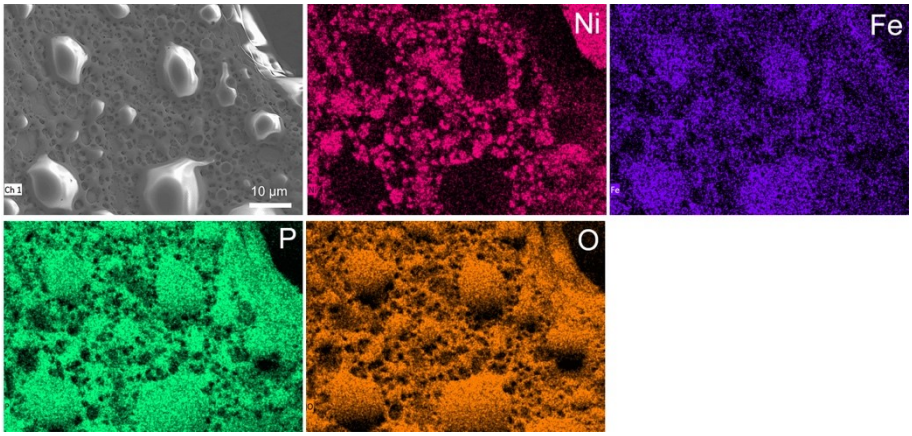

Figure S4. Elemental mapping images of corresponding elements of Ni, Fe, P, and O in L-FePO on NF.

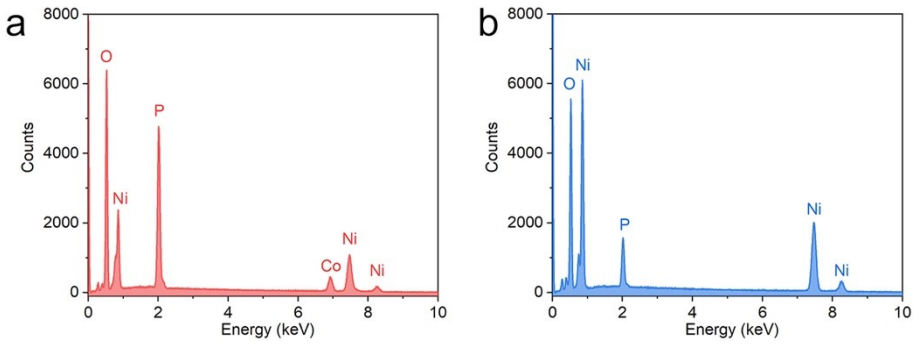

Figure S5. EDX spectra of (a) L-CoPO and (b) L-NiPO.

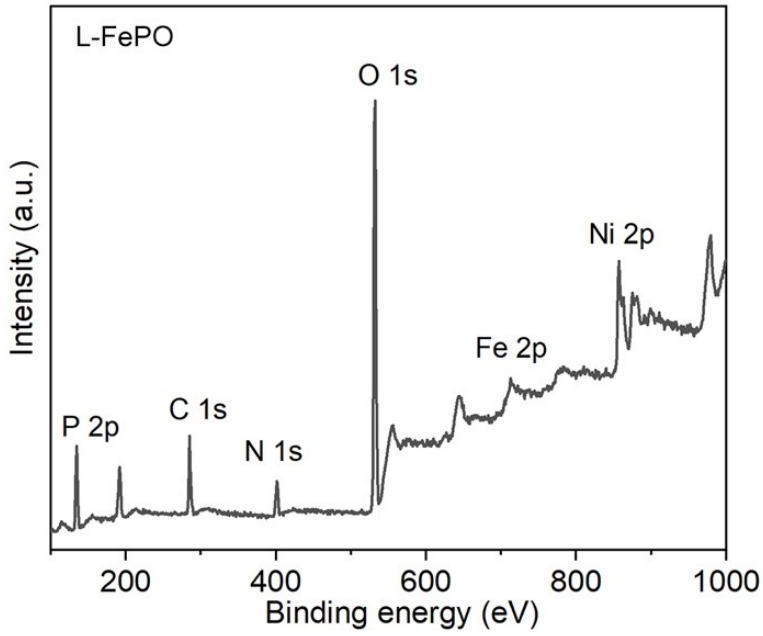

Figure S6. Full XPS spectrum of L-FePO on NF.

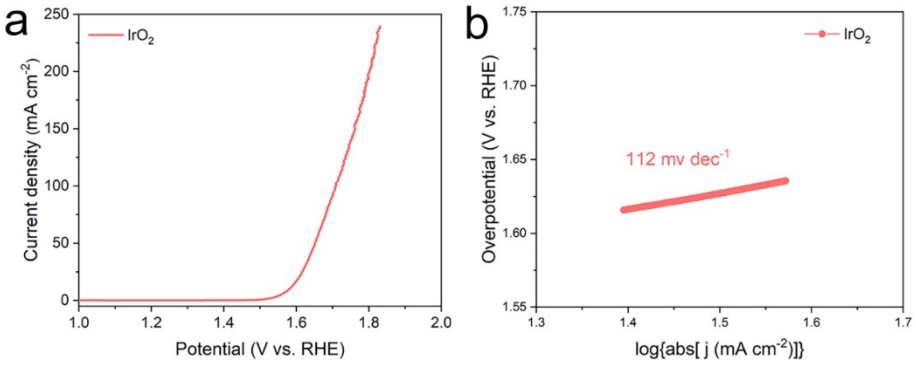

Figure S7. (a) LSV curve and (b) Tafel plot of the commercial IrO_2 catalyst for OER in an alkaline medium.

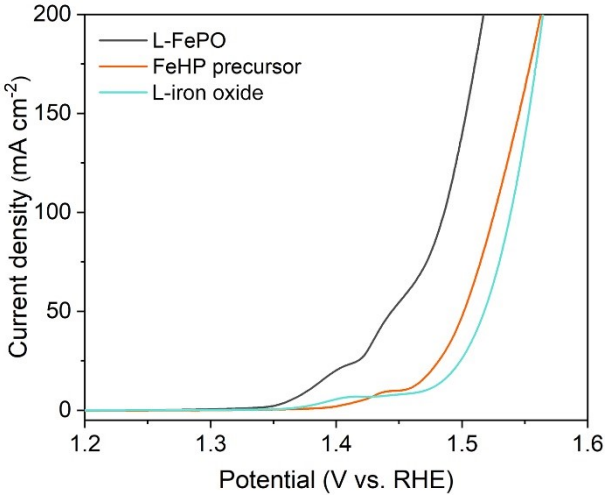

Figure S8. LSV curves of L-FePO, the FeHP precursor prepared using $Fe(NO_3)_3/NH_4H_2PO_4$ mixture, and L-iron oxide prepared by the direct laser-induced treatment of $Fe(NO_3)_3$ coated on NF.

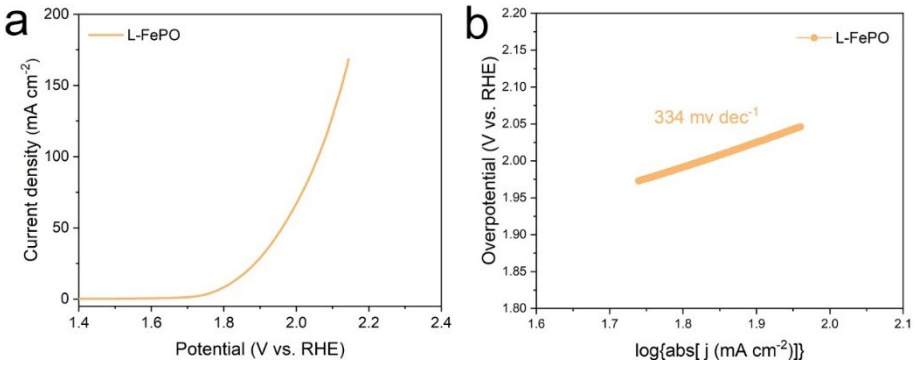

Figure S9. (a) LSV curve and (b) Tafel plot L-FePO on NF measured in 1.0 M PBS.

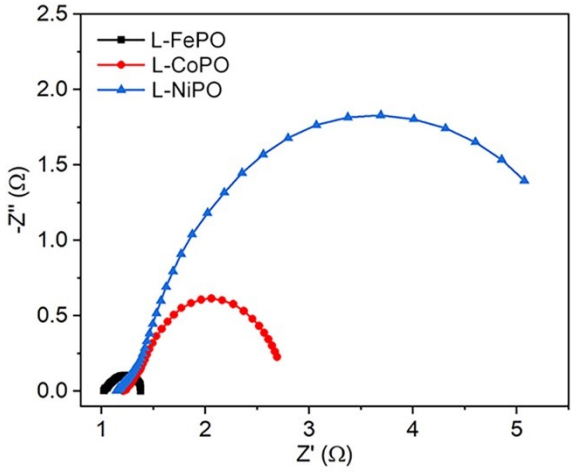

Figure S10. EIS spectra of L-FePO, L-CoPO, and L-NiPO on NF.

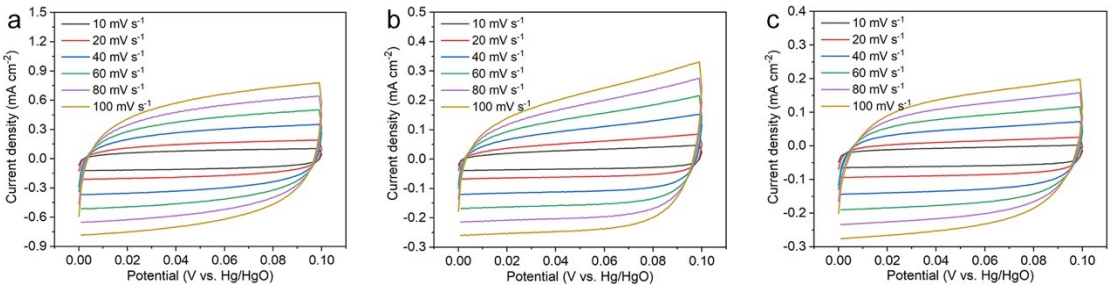

Figure S11. CV curves of (a) L-FePO, (b) L-CoPO, and (c) L-NiPO on NF measured in a non-faradic region of 0-0.1 V vs. Hg/HgO at different scan rates (10-100 mV s^{-1}).

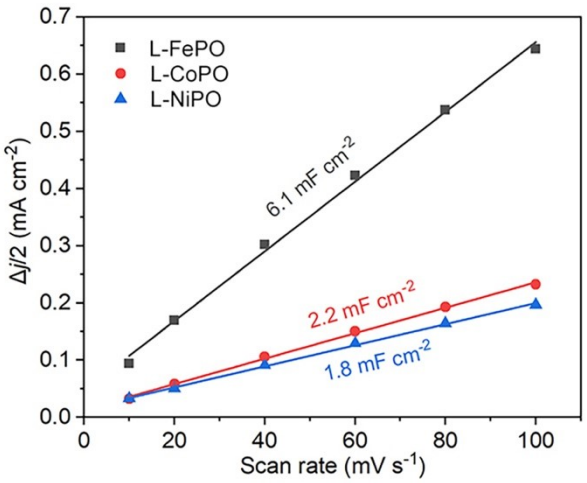

Figure S12. C_{dl} plots of L-FePO, L-CoPO, and L-NiPO on NF.

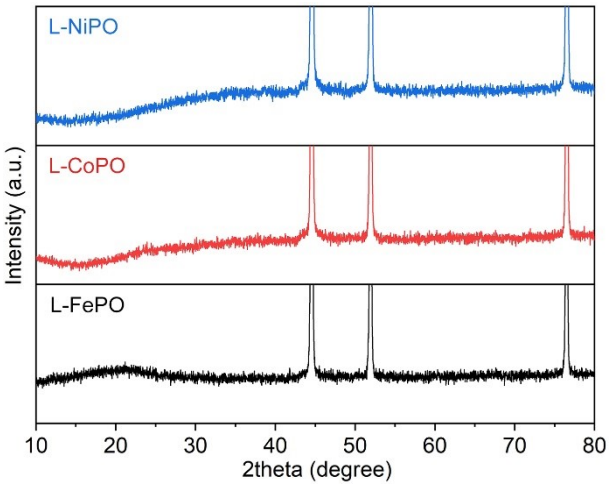

Figure S13. XRD patterns of L-MPO on NF after the stability test for OER

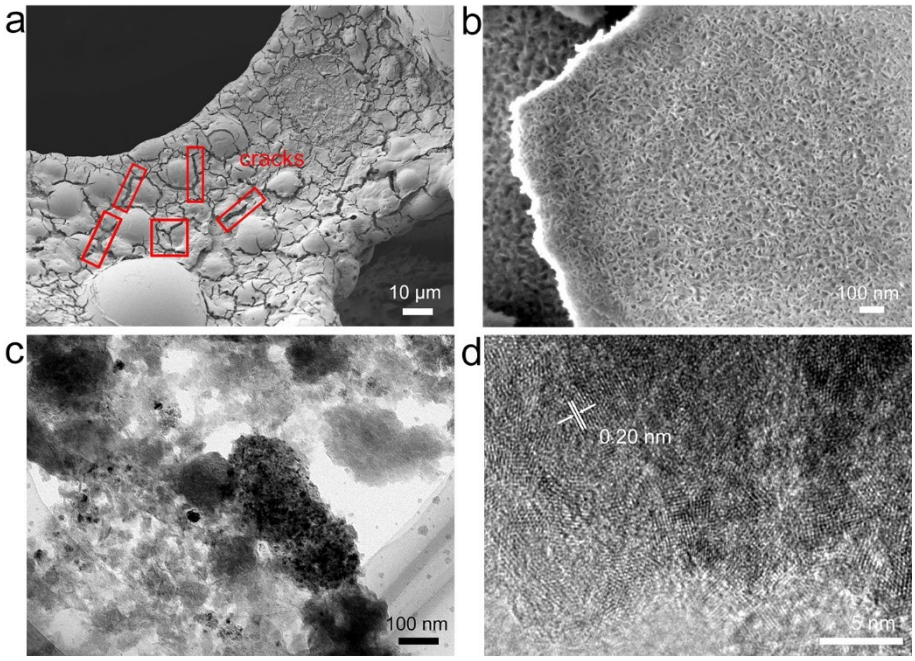

Figure S14. (a, b) SEM, (c) TEM, and (d) HRTEM images of L-FePO after the stability test for OER.

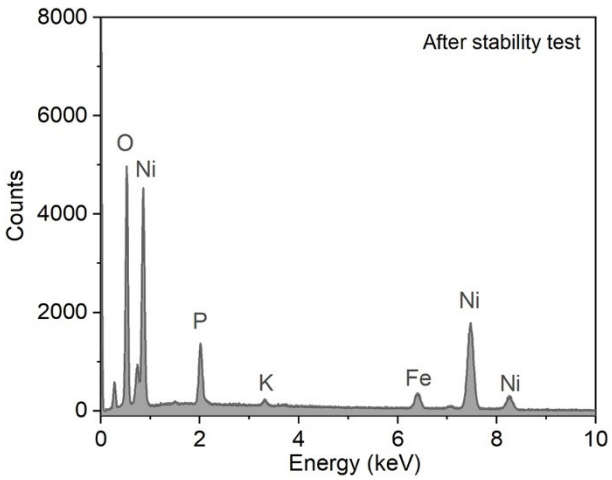

Figure S15. EDX spectra of L-FePO on NF after the stability test for OER in 1.0 M KOH.

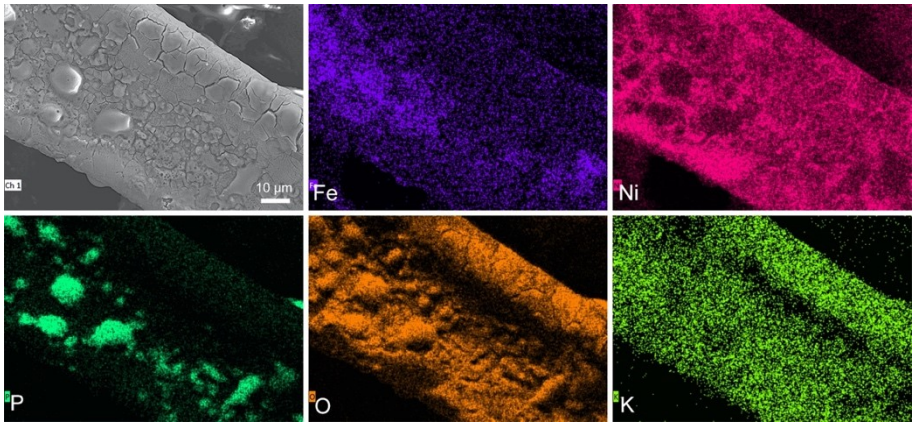

Figure S16. Elemental mapping images of L-FePO on NF after the stability test for OER.

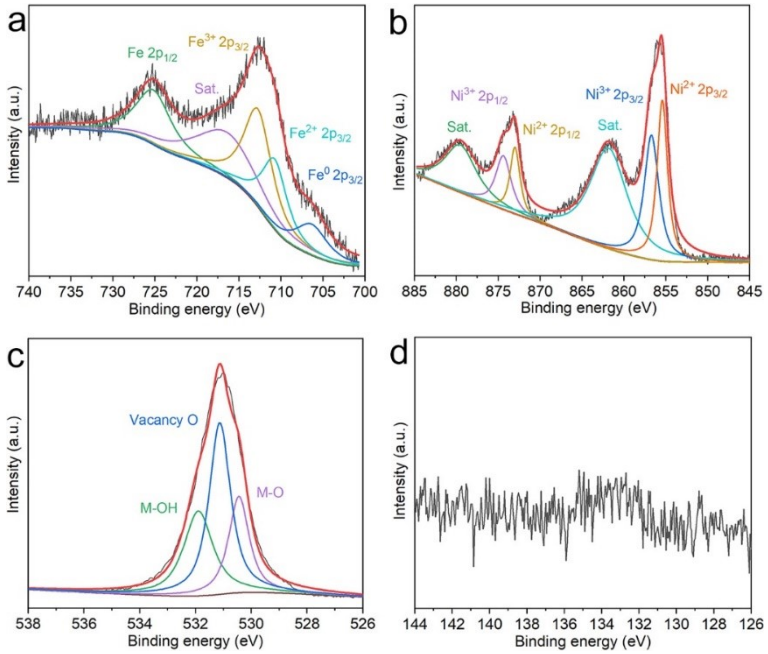

Figure S17. High-resolution XPS spectra of (a) Fe 2p, (b) Ni 2p, (c) O 1s, and (d) P 2p.

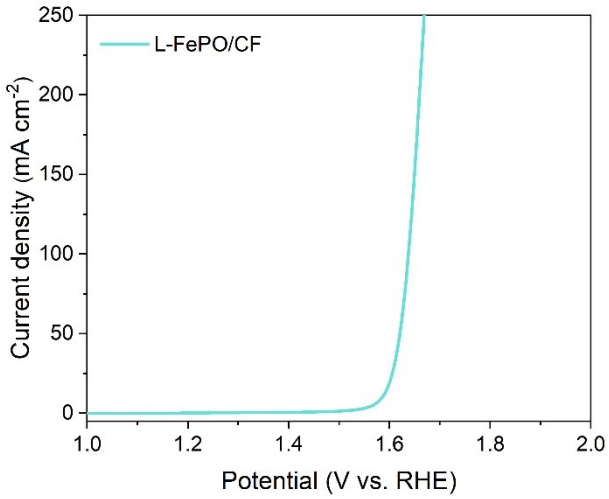

Figure S18. LSV curve of L-FePO laser-irradiated on Cu foam for OER in 1 M KOH.

The L-FePO composite laser-irradiated on the Cu foam (CF) substrate was applied to investigate the influence of Ni-doping orginating from the NF support. The LSV curves show that the η_{100} value of L-FePO on CF was 408 mV, which was higher than that of L-FePO on NF, suggesting its poor OER activity. Therefore, the Ni sources doped into L-FePO and the conductive NF support could enhance the electrocatalytic activity to some extent.

Table S1. OER comparison of L-MPO on NF and recently reported phosphate- and oxide-based electrocatalysts.

Electrocatalyst	Support	Electrolyte	Overpotential	Tafel slope (mV dec^{-1})	Reference
L-FePO	Ni foam	1 M KOH	256 mV @ 100 mA cm^{-2}	71	This work
P-CoPc@CNT	GCE[a]	1 M KOH	300 mV @ 10 mA cm^{-2}	41.7	1
2D-CoHPi	GCE	1 M KOH	314 mV @ 10 mA cm^{-2}	31	2
NiCo-LDH/NiCoPi	Ni foam	1 M KOH	300 mV @ 100 mA cm^{-2}	73	3
CoFeNiMnMoPi(HEPi)	GCE	1 M KOH	270 mV @ 10 mA cm^{-2}	74	4
$Fe_xNi_{2-x}P_4O_{12}$/RGO	GCE	1 M KOH	270 mV @ 10 mA cm^{-2}	43.8	5
N-$NiMoO_4$/Ni/CNTs	GCE	1 M KOH	330 mV @ 10 mA cm^{-2}	89.5	6
Fe–Co–O/Co@NC-mNS/NF	Ni foam	1 M KOH	257 mV @ 10 mA cm^{-2}	41.56	7
Co, S-Fe_3O_4/IF	Ni foam	1 M KOH	356 mV @ 10 mA cm^{-2}	50.9	8
Co_3O_4 nanomeshes	GCE	1 M KOH	307 mV @ 10 mA cm^{-2}	76	9
NiO_x-$NiSe_2$	GCE	1 M KOH	266 mV @ 10 mA cm^{-2}	53.4	10

Note: a) GCE denotes glassy carbon electrode.

Reference

1 Y. Liu, S. Zhang, C. Jiao, H. Chen, G. Wang, W. Wu, Z. Zhuo and J. Mao, *Adv. Sci.*, 2023, **10**, 2206107.

2 J. Wang and H. C. Zeng, *ACS Appl. Mater. Interfaces*, 2018, **10**, 6288-6298.

3 S. Zhou, Y. Liu, J. Li, Z. Liu, J. Shi, L. Fan and W. Cai, *Green Energy Environ.*, 2022, doi: https://doi.org/10.1016/j.gee.2022.12.003.

4 H. Qiao, X. Wang, Q. Dong, H. Zheng, G. Chen, M. Hong, C.-P. Yang, M. Wu, K. He and L. Hu, *Nano Energy*, 2021, **86**, 106029.

5 L. Lin, Y. Wang, Q. Ye, Y. Zhao and Y. Cheng, *Appl. Catal., B*, 2023, **334**, 122834.

6 G.-L. Li, X.-Y. Qiao, Y.-Y. Miao, T.-Y. Wang and F. Deng, *Small*, 2023, **19**, 2207196.

7 T. I. Singh, G. Rajeshkhanna, U. N. Pan, T. Kshetri, H. Lin, N. H. Kim and J. H. Lee, *Small*, 2021, **17**, 2101312.

8 H.-J. Liu, S. Zhang, Y.-N. Zhou, W.-L. Yu, Y. Ma, S.-T. Wang, Y.-M. Chai and B. Dong, *Small*, 2023, **19**, 2301255.

9 Y. Li, F.-M. Li, X.-Y. Meng, S.-N. Li, J.-H. Zeng and Y. Chen, *ACS Catal.*, 2018, **8**, 1913-1920.

10 H. Li, S. Chen, H. Lin, X. Xu, H. Yang, L. Song and X. Wang, *Small*, 2017, **13**, 1701487.